Physics Letters A 380 (2016) 3559–3563

Contents lists available at ScienceDirect

Physics Letters A

www.elsevier.com/locate/pla

Methylation effect on the ohmic resistance of a poly-GC DNA-like chain

F.A.B.F. de Moura [a,*,1], M.L. Lyra [a], M.L. de Almeida [b], G.S. Ourique [b], U.L. Fulco [b], E.L. Albuquerque [b]

[a] Instituto de Física, Universidade Federal de Alagoas, Maceió AL 57072-970, Brazil
[b] Departamento de Biofísica e Farmacologia, Universidade Federal do Rio Grande do Norte, 59072-970, Natal-RN, Brazil

ARTICLE INFO

Article history:
Received 9 May 2016
Received in revised form 13 July 2016
Accepted 25 July 2016
Available online 29 August 2016
Communicated by R. Wu

Keywords:
Tight-binding Hamiltonian
DNA Poly-GC finite segment
Methylated DNA
IxV characteristic curves

ABSTRACT

We determine, by using a tight-binding model Hamiltonian, the characteristic current–voltage (IxV) curves of a 5-methylated cytosine single strand poly-GC DNA-like finite segment, considering the methyl groups attached laterally to a random fraction of the cytosine basis. Striking, we found that the methylation significantly impacts the ohmic resistance (R) of the DNA-like segments, indicating that measurements of R can be used as a biosensor tool to probe the presence of anomalous methylation.

1. Introduction

Theoretical and experimental investigations of the electronic and optical properties of biological self-assembled systems have attracted a great interest in recent years (for reviews see Refs. [1–3]). In general, within the context of molecular electronics, they present a wide range of different effects induced by the electric fields due to the unusual quality and quantity of their electric parameters, as well as a consequence of their chemical modifications. [4,5].

As a bold example, the nucleic acids (DNA and RNA) and the proteins are not only biologically important polymers but also basic functional materials, surpassing the conventional one in many aspects due to its unique transport properties [6,7]. However, the possible manipulation of these biopolymers via their charge transport between two conducting electrodes is still a challenge open problem, with several possible applications in the field of nanoelectronic devices (for a review see Ref. [8]).

From the experimental point of view, some previous works have addressed the charge flow in DNA segments, unveiling important issues regarding their electrical conductivity [9–13]. On the other hand, theoretical investigations of the charge transport in DNA are being made by using a quantum formalism based on a single electron tight-binding Hamiltonian exploring its distinct aspects [14–18]. Focusing on the DNA case, the model consider Watson–Crick pairs attached to the sugar-phosphate backbone condensed into a single nucleotide site. Although it was successful employed to describe numerous experimental data [8], it has some critical assessment [19]. A relevant consideration is the topology of the double-helix, which is not a rigid object, with the different constituents of DNA moving relative to each other presenting linear deformations of its structure in response to the charge arrival at this particular site (polaronic effects) [20].

In general lines, the DNA Hamiltonian is constructed by assuming that the transmission channels are along their longitudinal axis, consisting of a π-stacked array of DNA nucleobases formed by a symbolic sequence of a four letters alphabet, namely guanine (G), adenine (A), cytosine (C) and thymine (T) [21,22]. It is important to emphasize that under this formalism, the effective model of real DNA segments corresponds to a low-dimensional disordered structure. Therefore, the electronic eigenstates become localized due to the scattering by the intrinsic disorder (Anderson localization), resulting in an insulator-like behavior [23].

Several mechanisms have been considered to provide a good understanding of the electronic transport properties of the DNA molecule, some of them related to the internal DNA correlations [24,25]. For instance, the presence of long-range correlations within the disorder distribution can promote electronic delocalization [26]. However, an instructive debate within the literature

* Corresponding author.
E-mail address: fidelis@fis.ufal.br (F.A.B.F. de Moura).
[1] Fax: +55 82 3214-1645.

http://dx.doi.org/10.1016/j.physleta.2016.07.069
0375-9601/

suggests that the type of correlations present in real DNA segments is not strong enough to play a major role in their electronic transport. Besides, disorder effects in synthetic DNA-segments can be minimized, opening up the way to tailor the electronic properties required to operate distinct device functions [27,28].

The focus of this work is on the investigation of the electronic charge transport properties in a poly-GC DNA segment. Specifically, we are interested to identify an electrical signature due to the presence of methyl groups randomly connected to the cytosine nucleobases in this structure, the so-called 5-methylcytosine, a well-studied epigenetic pathway implicated in gene expression control and disease pathogenesis. Usually, the 5-methylcytosine-based DNA methylation occurs through the covalent addition of a methyl group at the 5-carbon of the cytosine heterocyclic aromatic ring by an enzyme called DNA methyltransferase, a very important repressor of transcription in the human genome which contains over 60% repetitive DNA, much of which being transposable sequences of viral origin that are kept inactive in part by DNA methylation [29,30]. Unfortunately, a growing number of human diseases have been found to be associated with aberrant DNA methylation, leading to new and fundamental insights about the roles played by DNA methylation and other epigenetic modifications on the human genome in the form of epigenetic marks that are heritable during cell division but do not alter the DNA sequence [31].

One of the most complex and challenging question is how to detect small methylation fractions along DNA segments. Considering that, we set up here a quantum Hamiltonian approach to describe electronically a finite poly-GC segment with a variable methylation fraction p and nearest-neighbor hopping terms, to numerically compute its density of states, electronic transmittance profiles, and the current–voltage (IxV) characteristic curves, looking for a kind of signature that can be useful for the development of nanodevices as diagnostics tools for methylation-related diseases.

2. Theoretical model

Our theoretical model consists of a quantum one-dimensional tight-binding Hamiltonian describing a methylated single-strand poly-GC DNA sandwiched between two metallic electrodes, namely:

$$H = \sum_n \epsilon_n |n><n| + \sum_{(n,m)} t_{n,m}(|n><m| + c.c) + H_L + H_R. \quad (1)$$

Here, ϵ_n represents the on-site energy related to the poly-GC segment, (n,m) represents a sum over nearest-neighbor sites, and $t_{n,m}$ is the hopping term between the poly-GC DNA basis. Also H_L and H_R mean the quantum Hamiltonian describing the left and right metallic electrodes, respectively. Following [32], we will consider these electrodes as metallic systems whose Hamiltonians have diagonal ionization energy term $\epsilon_E = 5.36$ eV and non-diagonal internal hopping $t_E = 12$ eV. The coupling between the methylated single-strand poly-GC DNA and the semi-infinite metallic electrodes is measured by a hopping amplitude $t_{EP} = 0.63$ eV. The on-site distribution of the poly-GC segment is, from the theoretical point of view, an alternate sequence of cytosine (C) and guanine (G) basis, whose ionization energies (hopping amplitudes) are $\epsilon_C = 8.87$ eV and $\epsilon_G = 7.75$ eV ($t_{CG} = 0.282$ eV and $t_{GC} = 0.144$ eV). The 5-methylcytosine-based DNA methylation, taking into account the attachment of methyl groups in the 5-carbon of a random fraction p of the cytosine basis, is characterized by an ionization energy (hopping term) $\epsilon_M = 7.02$ eV ($t_{MG} = 0.145$ eV and $t_{GM} = 0.210$ eV).

Having defined the Hamiltonian model, we now briefly describe the methodology employed to investigate the electronic transport in a finite methylated synthetic poly-GC DNA segment with N basis, starting from the calculation of the electronic density of states of long segments (DOS) by using the Dean's method [33]. To do that, we solve the secular equation $\det(H_{GC} - EI) = 0$, where E is the eigenvalue, I is the identity operator, and H_{GC} is the Hamiltonian of the methylated poly-GC DNA segment, i.e., the Hamiltonian of eq. (1) without the electrodes terms.

Defining a polynomial $g_m(E)$ (with $m = 1, ..., N$, N being the number of nucleobases), such that $g_N(E) = \det(H_{GC} - EI)$, the use of the co-factors method yields $h_m(E) = E - \epsilon_M - t_{MG}^2/h_{m-1}$, where $h_m = g_m(E)/g_{m-1}(E)$. The integrated density of states ($IDOS$) then follows by taking into account the signal changes in the set of the h_m functions. Furthermore, the density of states (DOS) is thus obtained by using a simple direct numerical derivative $DOS = d(IDOS)/dE$.

Due to the random nature of methylation of cytosine sites, the electronic eigenstates become exponentially localized (Anderson localization) on very long single strand DNA's geometry, strongly suppressing its electronic transmission spectrum. However, finite transmission can still be achieved in shorter DNA's segments associated to the presence of resonant states. In what follows, we will explore the electronic transmission spectra by considering a shorter DNA's finite segment with $N = 30$ bases, closer to the realistic size of a DNA primer, which is a short single strand structure that serves as a starting point for the DNA synthesis. For such realistic DNA's segments, the DOS is composed of a sequence of delta-like peaks signaling the eigenstates of the finite Hamiltonian matrix.

The transmission coefficient is computed by considering a plane wave being injected at one of the ends of the methylated poly-GC single strand segment. The transmission coefficient $T_N(E)$, that gives the transmittance spectra through the chain and is related to the Landauer resistance, is then defined by [21]:

$$T_N(E) = (4 - X^2(E))\Big[-X^2(E)(\mathcal{P}_{12}\mathcal{P}_{21} + 1) + X(E)(\mathcal{P}_{11} - \mathcal{P}_{22})(\mathcal{P}_{12} - \mathcal{P}_{21}) + \sum_{i,j=1,2} \mathcal{P}_{ij}^2 + 2\Big]^{-1}, \quad (2)$$

where $X(E) = (E - \epsilon_j)/t_j$, and $\mathcal{P}_{ij}$ are elements of the transfer matrix $\mathcal{P} = M(N+1)M(N-1)\cdots M(2)M(1)M(0)$, with [34]

$$M(j) = \begin{pmatrix} X(E) & -t_{j-1}/t_j \\ 1 & 0 \end{pmatrix}. \quad (3)$$

Here the matrix $M(j)$ is computed using the methylated poly-GC segment. Also, $M(0)$ and $M(N+1)$ represent the local transfer matrix related to the contacts at the ends of the poly-GC DNA model. For a given energy E, $T_N(E)$ measures the level of backscattering events for electrons (or holes) transport through the chain.

The transmission coefficient $T_N(E)$ is a useful quantity to describe the transport efficiency in quantum systems. However, from the experimental point of view, the electronic transport properties are more easily investigated by measuring their current–voltage (IxV) characteristics curves. The theoretical calculation of the IxV curves can be done by applying the Landauer–Büttiker formulation [35,36], i.e.:

$$I(V) = \frac{2e}{h} \int_{-\infty}^{+\infty} T_N(E)[f_L(E) - f_R(E)]dE, \quad (4)$$

where $f_{L(R)}(E)$ is the Fermi–Dirac distribution at the left (right) side of the electrodes, i.e.:

$$f_{L(R)} = \Big[\exp[(E - E_F \mp eV/2)/k_BT] + 1\Big]^{-1}. \quad (5)$$

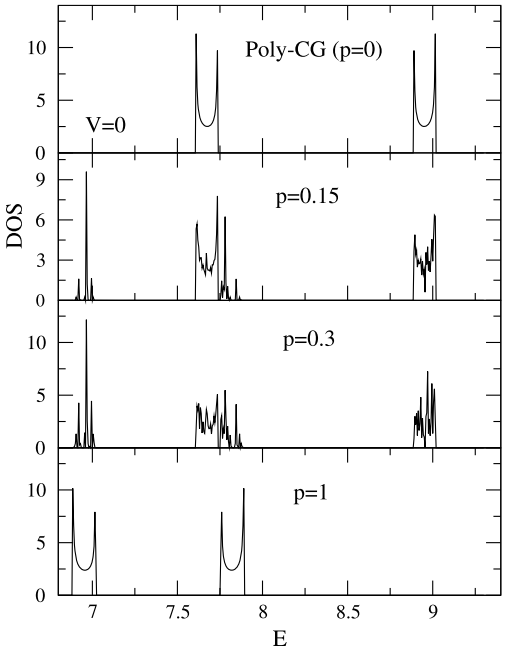

Fig. 1. Electronic density of states (DOS) calculated by using the Dean's method for a long single-strand methylated poly-GC segments with $N = 10^5$ and methylation fractions $p = 0$, 0.15, 0.3, and 1.0. For $p = 0$ and $p = 0$, the DOS exhibits two sub-bands around $E \approx \epsilon_C$ and ϵ_G ($p = 0$) and $E \approx \epsilon_M$ and ϵ_G ($p = 1$), i.e. profiles quite compatible with a crystalline chain with two distinct atoms within the unitary cell. We also observe that the DOS of the non-methylated and fully methylated segments exhibit smooth profiles. For $0 < p < 1$, a finite fraction of the cytosine nucleobases suffers the methylation process, and the DOS smooth profile is degraded by the presence of the disorder.

The Fermi level energy E_F is properly located at the lowest characteristic resonances of the electrode—5-methylcytosine-based DNA methylatione—electrode nano-junction, namely the ionization energy of the guanine ϵ_G. Besides, we have considered $T = 310$ K (the mean body temperature) in such a way that the thermal energy $k_B T << E_F$. The resulting IxV curves then will correspond to the low-temperature regime of the conducting electrons.

In order to calculate the IxV profiles, the transmission coefficient will be considered to be bias-dependent by assuming that the potential energy at one of the ends is $\epsilon_E^* = 5.36 + eV$ (in units of electron-volts), where V represents the voltage and e the electron charge. Further details of the above methodology can be found in [37–39].

3. Results and discussions

The Dean's method is computationally efficient and allows us to calculate the electronic density of states (DOS) for large methylated poly-GC segments. In our calculations we used $N = 10^5$ basis in order to clearly unveil the methylation influence on the DOS profile, as depicted in Fig. 1 which shows a normalized electronic density of states versus the energy E for the methylation fractions $p =$ 0, 0.15, 0.3 and 1.0. We emphasize that the case $p = 0$ represents a crystalline poly-GC segment with no methylated cytosine sites, while for $p > 0$ a finite fraction of cytosine suffers the methylation process. $p = 1$ stands for the fully methylated chain. Observe that for the non-methylation ($p = 0$) and fully methylated ($p = 1$) cases, the DOS exhibits a profile quite compatible to crystalline chains with two distinct atoms within the unitary cell. Indeed, two sub-bands are found around E approximately equal to the ionization energies of the cytosine and guanine basis for $p = 0$ and around the methylated cytosine and guanine basis for $p = 1$. Furthermore, the electronic density of states exhibits a smooth

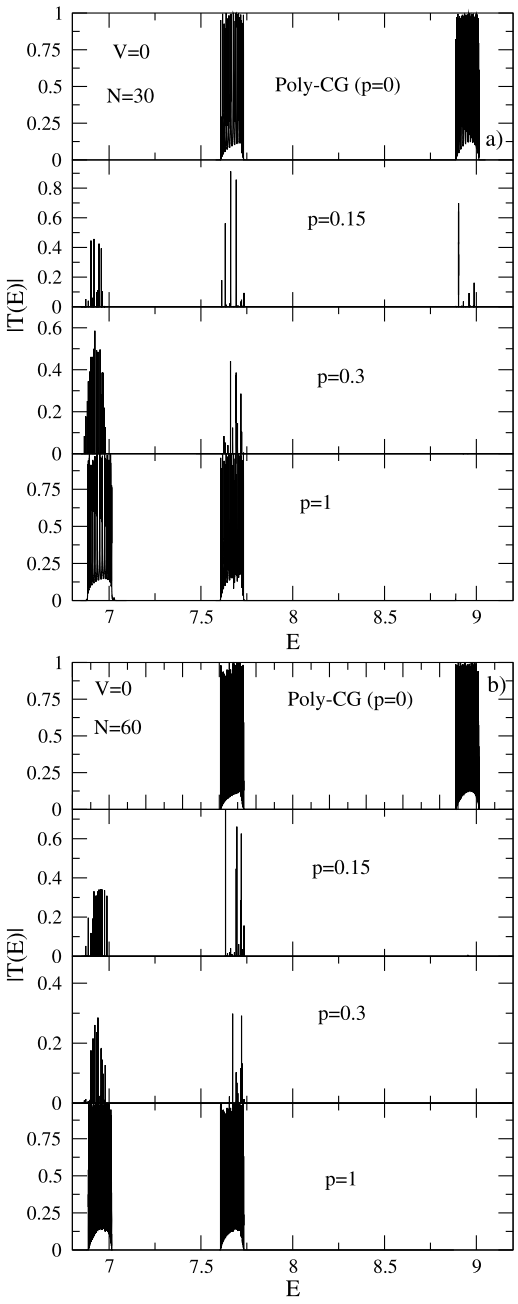

Fig. 2. Transmission coefficient $T_N(E)$ versus the energy E for: (a) $N = 30$, $V = 0$ and methylation fractions p=0, 0.15, 0.3 and 1.0; (b) as in (a) but considering $N = 60$. For $p = 0$ and $p = 1$ the transmission coefficient is close to unity within the bands of allowed energies, in good agreement with the crystalline behavior of the poly-GC and poly-GM chains. For $0 < p < 1$ the presence of a finite fraction of methylated cytosine decreases the electronic transmission due to the intrinsic disorder characteristic of the methylated poly-GC chain.

profile with typical Van Hove singularities of translational invariant crystalline systems. The smoothness of the DOS results from the effective level repulsion of the extended energy eigenstates. When methylation occurs ($0 < p < 1$) the smooth profile of the DOS is degraded since the presence of methyl groups randomly distributed along the chain introduces a small disorder distribution. Therefore, under the presence of disorder, one-dimensional systems exhibit localized states and the DOS displays a rough profile, a signature of the absence of level repulsion for exponentially localized states [40].

Fig. 2(a) presents the transmission coefficient $T_N(E)$ versus energy E for the case where there is no bias voltage V by considering

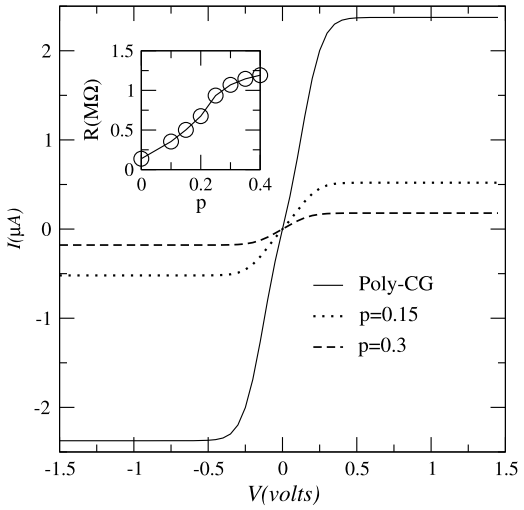

Fig. 3. Current–Voltage (IxV) curves computed by using the Landauer–Büttiker formalism. The curves exhibit a strong dependence on the methylation fractions p. As we increase their concentration the saturation current I_{sat} substantially decreases, detecting the methylation within the poly-GC segments. Inset: the effective ohmic resistance R (in $M\Omega$) versus the concentration of the methylation fraction p. We measure R by computing the numerical derivative dV/dI around $V = 0$.

the number of nucleobases $N = 30$, and the methylation fractions $p = 0$, 0.15, 0.3 and 1.0. For comparison, Fig. 2(b) depicts the case in which the number of nucleobases $N = 60$. The average transmission becomes small at longer chains due to the Anderson localization of the energy eigenstates. In short chains, the transmission peaks reflect the presence of resonant states. Our results for $p = 0$ (i.e. the crystalline poly-GC model) are in good agreement with similar calculations found in the literature [37–39]. We emphasize that the specific parameter set used here is an intrinsic characteristic of the modeled system. However, despite the set of values considered, the periodic poly-GC model represents a crystalline system, and high electronic transmission can be readily anticipated. As one can see in Figs. 2(a) and 2(b), the transmission coefficient $T_N(E)$ is in fact close to unity for the pure poly-GC case (no methylation fraction, i.e., $p = 0$) as well as for the pure poly-GM chain $p = 1$ within the nads of allowed energies. As we increase the concentration of methylated cytosines ($0 < p < 1$), one can observe a considerable deterioration of the degree of transmittance, although some resonant modes appears around the on-site energy of the methylated cytosine as a precursor of the low energy transmission band that sets up at $p = 1$. For $0 < p < 1$, the poly-GC DNA structure loses its translational invariance, becoming a disordered chain. Therefore, the eigenstates become exponentially localized and the transmission coefficient $T_N(E)$ decreases as the system size N is increased. Notice that the sub-band with energies around the cytosine's ionization energy ϵ_C feels more drastically the effect of the presence of methylated cytosine sites. We can understand this feature by recalling that the high-energy eigenmodes are more sensitive to the presence of disorder. Therefore, the transmission band around ϵ_M develops quickly as p increases while the transmission band around ϵ_c is rapidly degraded.

As evidenced above, both the electronic density of states and the transmission coefficient exhibit a great sensibility in the presence of the methylated cytosine concentration p, being useful to detect the presence of methylation within poly-GC segments. However, current–voltage (IxV) curves are the usual experimental quantifiers of electronic transport characteristics, as depicted in Fig. 3, considering the unity of the computed current (bias) μA (Volt). We have taken $N = 30$ basis and distinct methylation fractions p, setting the Fermi level within the first sub-band ($E_F = \epsilon_G$). Therefore, the transmission coefficient, although small, is not null for $p > 0$, leading to a finite transmission near the Fermi level, and thus promoting an ohmic behavior for small voltages V.

By further analyzing the IxV characteristic curves depicted in Fig. 3, we observe this ohmic behavior close to the zero bias region characterized by a linear curve $I(V) = -I(-V)$, besides a strong sensitivity to the presence of the methylated cytosine concentration. As we increase the methylation fraction p, the current $I(V)$ decreases, implying that the IxV curves can probe methylation in poly-GC segments. Note that the current saturates in the large bias regime in which electrons in the entire conducting band contribute. The saturation current decreases by approximately one order of magnitude for a $p = 0.3$ methylation fraction.

In the inset of Fig. 3, we plot the effective ohmic resistance R (in $M\Omega$) versus the concentration of methylated cytosine p, by computing the numerical derivative dV/dI around $V = 0$. Our results show clearly the sensitivity of the electric conductance of poly-GC segments regarding the presence of the methylated cytosine concentration, with the resistance also changing up to one order of magnitude. It saturates at a maximum value and decreases for larger methylation fractions. This feature is related to the fact that the system recovers its periodicity when all cytosine basis are methylated. Therefore, IxV curves and localization characteristics may be an useful tool to detect the presence of methylated cytosine in DNA-like segments, being a kind of important signature for methylation-related diseases.

4. Summary and conclusions

In summary, we investigated some electronic transport characteristics of a single-strand methylated poly(GC) DNA segment considering the possibility that methyl groups can be attached to a finite fraction of the cytosine sites in a random way. After the methyl group is attached to a specific cytosine, both its ionization energy and nearest neighbor hopping are modified. Our main aim was the investigation of the effects of methylated cytosine concentration on the electronic transport along poly(GC) DNA-like segments, modeling this system by a quantum one-electron Hamiltonian containing nearest-neighbor hoppings, as well as the on-site poly-GC basis ionization energies.

Our results suggest that the localization properties, as well as the IxV curves, may be used as an important biosensor to detect the presence of methylated cytosines, which considerably degrade the electronic transport in poly-GC chains. We numerically demonstrated that the effective resistance of methylated synthetic poly-GC segments increases by up to one order of magnitude when the concentration of the methylated cytosine p is increased. Considering that methylation is an important mechanism related to several biological processes, the present results suggest that measurements of standard electronic characteristics can be used as a suitable witness of methylation in DNA segments.

Acknowledgements

This work was partially financed by the Brazilian Research Agencies CAPES (PROCAD), CNPq (INCT-Nano(Bio)Simes, Procad-Casadinho), FAPERN, and FAPEAL.

References

[1] H.-A. Wagenknecht (Ed.), Charge Transfer in DNA: From Mechanism to Application, Wiley, New York, 2005.
[2] G. Cuniberti, E. Maciá, A. Rodriguez, R.A. Römer, in: T. Chakraborty (Ed.), Charge Migration in DNA: Perspectives from Physics, Chemistry and Biology, Springer, Berlin, 2007.
[3] J.K. Barton, A.L. Furst, M.A. Grodick, in: E. Stultz, G.H. Clever (Eds.), DNA in Supramolecular Chemistry and Nanotechnology, Wiley, New York, 2015.
[4] I. Kratochvilova, K. Kral, M. Buncek, A. Viskova, S. Nespurek, A. Kochalska, T. Todorciuc, M. Weiter, B. Schneider, Biophys. Chem. 138 (2008) 3–10.

[5] D. Porschke, Biophys. Chem. 66 (1997) 241–257.
[6] J.I.N. Oliveira, E.L. Albuquerque, U.L. Fulco, P.W. Mauriz, R.G. Sarmento, Chem. Phys. Lett. 612 (2014) 14.
[7] L. Xiang, J.L. Palma, C. Bruot, V. Mujica, M.A. Ratner, N. Tao, Nat. Chem. 7 (2015) 221.
[8] E.L. Albuquerque, U.L. Fulco, V.N. Freire, E.W.S. Caetano, M.L. Lyra, F.A.B.F. de Moura, Phys. Rep. 535 (2014) 139.
[9] D. Porath, A. Bezryadin, S. De Vries, C. Dekker, Nature 403 (2000) 635.
[10] B. Xu, P. Zhang, X. Li, N. Tao, Nano Lett. 4 (2004) 1105.
[11] X. Guo, A.A. Gorodetsky, J. Hone, J.K. Barton, C. Nuckolls, Nat. Nanotechnol. 3 (2008) 163.
[12] J.D. Slinker, N.B. Muren, S.E. Renfrew, J.K. Barton, Nat. Chem. 3 (2011) 228.
[13] M.A. Grodick, N.B. Muren, J.K. Barton, Biochemistry 54 (2015) 962.
[14] C.R. Treadway, M.G. Hill, J.K. Barton, Chem. Phys. 281 (2002) 409.
[15] C.M. Chang, A.H. Castro Neto, A.R. Bishop, Chem. Phys. 303 (2004) 189.
[16] E. Diaz, F. Dominguez-Adame, Chem. Phys. 365 (2009) 24.
[17] R.G. Sarmento, E.L. Albuquerque, P.D. Sesion Jr, U.L. Fulco, B.P.W. de Oliveira, Phys. Lett. A 373 (2009) 1486.
[18] L.M. Bezerril, D.A. Moreira, E.L. Albuquerque, U.L. Fulco, E.L. de Oliveira, J.S. de Sousa, Phys. Lett. A 373 (2009) 3381.
[19] M.W. Shinwari, M.J. Deen, E.B. Starikov, G. Cuniberti, Adv. Funct. Mater. 20 (2010) 1865–1883.
[20] Y. Wang, L. Fu, K.L. Wang, Biophys. Chem. 119 (2006) 107–114.
[21] E.L. Albuquerque, M.S. Vasconcelos, M.L. Lyra, F.A.B.F. de Moura, Phys. Rev. E 71 (2005) 021910.
[22] E.L. Albuquerque, M.L. Lyra, F.A.B.F. de Moura, Physica A 370 (2006) 625.
[23] F.A.B.F. de Moura, M.L. Lyra, E.L. Albuquerque, J. Phys. Condens. Matter 20 (2008) 075109.
[24] F.A.B.F. de Moura, U.L. Fulco, M.L. Lyra, F. Domínguez-Adame, E.L. Albuquerque, Physica A 390 (2011) 535.
[25] M.O. Sales, U.L. Fulco, M.L. Lyra, E.L. Albuquerque, F.A.B.F. de Moura, J. Phys. Condens. Matter 27 (2015) 035104.
[26] F.A.B.F. de Moura, M.L. Lyra, Phys. Rev. Lett. 81 (1998) 3735.
[27] A. Sedrakyan, F. Domínguez-Adame, Phys. Rev. Lett. 96 (2006) 059703.
[28] R.C.P. Carvalho, M.L. Lyra, F.A.B.F. de Moura, F. Domínguez-Adame, J. Phys. Condens. Matter 23 (2011) 175304.
[29] M. Corbella, A.A. Voityuk, C. Curutchet, J. Phys. Chem. Lett. 6 (2015) 3749–3753.
[30] S. Nishikori, K. Shiraki, S. Fujiwara, T. Imanaka, M. Takagi, Biophys. Chem. 116 (2005) 97–104.
[31] K.D. Robertson, Nat. Rev. Genet. 6 (2005) 597.
[32] M.L. de Almeida, J.I.N. Oliveira, J.X. Lima Neto, C.E.M. Gomes, U.L. Fulco, E.L. Albuquerque, V.N. Freire, E.W.S. Caetano, F.A.B.F. de Moura, M.L. Lyra, Appl. Phys. Lett. 107 (2015) 203701.
[33] P. Dean, Rev. Mod. Phys. 44 (1972) 127.
[34] R.G. Sarmento, U.L. Fulco, E.L. Albuquerque, E.W.S. Caetano, V.N. Freire, Phys. Lett. A 375 (2011) 3993.
[35] R. Landauer, IBM J. Res. Dev. 1 (1957) 223.
[36] M. Büttiker, Phys. Rev. B 35 (1987) 4123.
[37] E. Maciá, Phys. Rev. B 76 (2007) 245123.
[38] E. Maciá, Phys. Rev. B 74 (2006) 245105.
[39] E. Maciá, F. Triozon, S. Roche, Phys. Rev. B 71 (2005) 113106.
[40] A.D. Mirlin, Phys. Rep. 326 (2000) 259.